Journal of Inorganic Biochemistry 194 (2019) 223–232

Contents lists available at ScienceDirect

Journal of Inorganic Biochemistry

journal homepage: www.elsevier.com/locate/jinorgbio

Flexible *vs.* rigid bis(2-benzimidazolyl) ligands in Cu(II) complexes: Impact on redox chemistry and oxidative DNA cleavage activity

Julian Heinrich[a], Niklas F. König[a,b], Sebastian Sobottka[a], Biprajit Sarkar[a], Nora Kulak[a,*]

[a] Institut für Chemie und Biochemie, Freie Universität Berlin, Fabeckstr. 34/36, 14195 Berlin, Germany
[b] Institut für Chemie, Humboldt-Universität zu Berlin, Brook-Taylor-Str. 2, 12489 Berlin, Germany

ARTICLE INFO

Keywords:
Cu(II) complexes
Metallonucleases
Bis(2-benzimidazolyl) ligands
DNA cleavage
Reactive oxygen species
DNA binding

ABSTRACT

Cu(II) complexes of bis(2-benzimidazolyl) ligands connected by different linker moieties (disulfide, ethylene, *ortho*-phenylene) were applied in DNA cleavage reactions. Hydroxyl radicals and hydrogen peroxide were proven as reactive oxygen species (ROS) in a DNA quenching experiment. Thus, an oxidative DNA cleavage mechanism is suggested. The binding affinity of the Cu(II) complexes to DNA was studied by UV–VIS (DNA melting), fluorescence (ethidium bromide displacement assay) and circular dichroism (CD) spectroscopy indicating a correlation between DNA binding and DNA cleavage efficiency. The most important finding was that oxidative nuclease activity correlated with flexibility of the linker between the benzimidazole moieties. A more flexible linker allowed for an easier switch between square planar (Cu(II)) and tetrahedral geometry (Cu(I)) for the complex, and thus resulted in an enhanced ROS generation. EPR spectroscopy and cyclic voltammetry were applied to investigate such changes in geometry and redox state.

1. Introduction

In the last twenty years bis(2-benzimidazoles) and bis(2-benzimidazolyl) alkanes have played an important role in research due to their broad field of application. Derivatives of these compounds have been investigated for their potential application in ion-exchange resins for selective uptake of Cu(II) [1,2], as polymerization catalysts [3,4] as well as in proton sponges [5] and electron transfer agents [6]. Bis(2-benzimidazoles) and bis(2-benzimidazolyl) alkane scaffolds have been used for the design of therapeutic agents due to their anti-inflammatory and analgesic properties [7,8]. When derivatives with different linker lengths were compared, a correlation between DNA binding affinity and antigiardial/antimicrobial activity was observed [9–11]. Additionally, Mo(V) complexes with bis(2-benzimidazolyl) alkane ligands exhibited enhanced activity against *E. coli* when compared to their ligands [12]. Presumably, the combination of a metal ion having an intrinsic high binding affinity to DNA with this class of biologically active ligands is promising for the design of artificial nucleases.

In medicinal inorganic chemistry, the application of artificial nucleases plays a key role for the development of novel chemotherapeutic agents [13,14]; the binding of which to DNA can be due to electrostatic interactions of (mostly) positively charged metal complexes with the negatively charged phosphate backbone, and π-stacking interactions between a planar aromatic ring of the ligand system and the DNA bases [15]. Due to the thus ensured spatial proximity, the artificial nuclease is able to cleave DNA efficiently through close-by generation of reactive oxygen species (ROS) in the case of an oxidative pathway [16–18].

It is known that Cu(II) complexes with various *N*-donor ligands can act as artificial nucleases by causing oxidative DNA cleavage [19]. Concerning the benzimidazole ligand moiety as an *N*-donor ligand, DNA cleavage has only been investigated with Cu(II) complexes comprising of bis(benzimidazol-2-ylmethyl)amine and mono(benzimidazol-2-yl) derivatives, respectively [20,21]. Due to the structural analogy of bis(2-benzimidazole) to the purines of nucleobases a strong DNA binding and consequently a high nuclease activity is anticipated [22].

Within the scope of this work the synthesis of three bis(2-benzimidazolyl) ligands comprised of disulfide, ethylene, and *ortho*-phenylene linkers, respectively, 1,2-bis(2-benzimidazolyl) disulfide (bimzS), 1,2-bis(2-benzimidazolyl) ethane (bimzE) and 1,2-bis(2-benzimidazolyl) benzene (bimzB), and their respective Cu(II) complexes $[Cu(bimzS)_2](NO_3)_2$ **1**$(NO_3)_2$, $[Cu(bimzE)_2](ClO_4)_2$ **2**$(ClO_4)_2$ and $[Cu(bimzB)_2](NO_3)_2$ **3**$(NO_3)_2$ (Fig. 1) was achieved. The ability of ligands and complexes to bind and cleave DNA was investigated applying various experimental techniques. Although two out of the three complexes have been described in the literature before [23,24], we have now, for the first time, thoroughly investigated the redox chemistry of these complexes and their biological activity (DNA binding and cleavage). The most important feature we have been investigating is the dependence of

* Corresponding author.
E-mail address: nora.kulak@fu-berlin.de (N. Kulak).

https://doi.org/10.1016/j.jinorgbio.2019.01.016
Received 27 August 2018; Received in revised form 27 January 2019; Accepted 27 January 2019
Available online 29 January 2019
0162-0134/

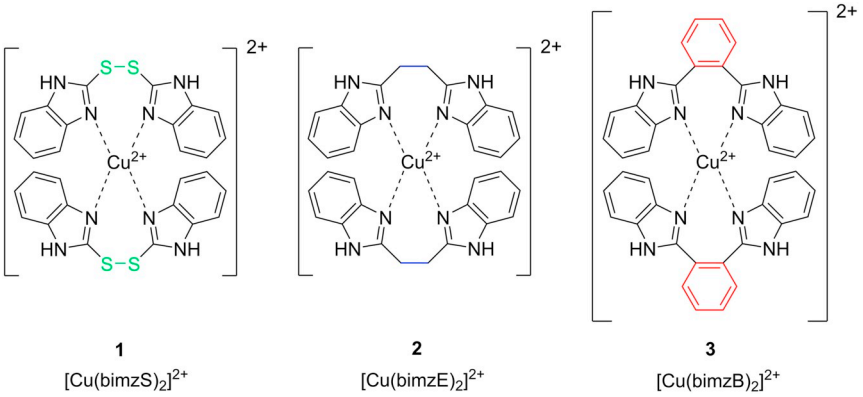

Fig. 1. Cu(II) complexes $[Cu(bimzS)_2]^{2+}$ (**1**) and $[Cu(bimzE)_2]^{2+}$ (**2**) with more flexible ligands bimzS and bimzE, and the Cu(II) complex $[Cu(bimzB)_2]^{2+}$ (**3**) with rigid, twisted V-shaped distorted ligands bimzB. Anions and solvent molecules are omitted for clarity.
For **2** and **3**, the structural formulas are based on reported solid-state molecular structures [23,24], whereas the structural formula of **1** is derived from analytical data presented herein.

redox chemistry, and consequently, oxidative DNA cleavage activity on the linker used between the benzimidazole moieties.

2. Experimental part

2.1. Materials and general methods

All chemicals and solvents were purchased from Sigma Aldrich, Merck, Fisher Scientific, Acros Organics and Carl Roth, respectively, and were used without further purification. ^{1}H NMR spectra of the ligands were recorded in acetone-d_6 and DMSO-d_6, respectively, on a Jeol ECX 400 spectrometer at room temperature. Chemical shifts are given relative to TMS with positive δ values indicating a low field shift. The characterization of the ligands and their Cu(II) complexes was performed *via* elemental analysis on a varioEL CHNS instrument. UV–VIS spectroscopy was carried out on a Varian Cary 100 Bio UV–VIS spectrophotometer.

2.2. Synthesis of the ligands

bimzS was prepared from 1,2-diaminobenzene in two steps *via* 2-thiobenzimidazole [25] and subsequent oxidation [26]. bimzE was synthesized by condensing 1,2-diaminobenzene with succinic acid according to literature reports in a two-step synthesis [27,28]. bimzB was prepared by a condensation reaction between 1,2-diaminobenzene and phthalic acid according to a literature method [23] (*cf.* S1).

2.3. Synthesis of the Cu(II) complexes

The Cu(II) complexes were prepared based on literature reports for the synthesis of the compounds $[Cu(bimzE)_2](ClO_4)_2$, abbreviated **2**$(ClO_4)_2$, and $[Cu(bimzB)_2](NO_3)_2$, abbreviated **3**$(NO_3)_2$ [23,24] (*cf.* S2).

2.4. Electrospray ionization mass spectrometry (ESI-MS)

The characterization of the ligands and their Cu(II) complexes was carried out on an Agilent 6210 ESI-TOF mass spectrometer using MeOH for the ligands and MeOH or MeCN for the complexes (flow rate 10 µL/min).

In situ stock solutions of **1**Cl_2, **2**Cl_2 and **3**Cl_2 were prepared similarly to the sample preparation for DNA cleavage incubation (*cf.* 2.8 and 3.6.1), but with the complexes 4× higher concentrated (0.4 mM) and MOPS (3-(*N*-morpholino)propanesulfonic acid) buffer 10× lower concentrated (5 mM). The samples were diluted with MeCN before measurement.

2.5. Electron paramagnetic resonance (EPR) spectroscopy

EPR spectra at X-band frequency (*ca.* 9.5 GHz) were obtained with a Magnettech MS-5000 benchtop EPR spectrometer equipped with a rectangular TE 102 cavity and TC HO4 temperature controller. The measurements were carried out in synthetic quartz glass tubes. The spectra were recorded with ESRStudio Version 1.20.6, further processing was done with OriginPro 2016G. The complex concentrations were about 10^{-2} M in an EtOH/MeCN mixture (2:1).

2.6. Cyclic voltammetry (CV)

Cyclic voltammograms were recorded with a PAR VersaStat 4 potentiostat (Ametek) by working in an anhydrous and degassed EtOH/MeCN mixture (2:1) with 0.1 M NBu_4PF_6 (dried, > 99.0%, electrochemical grade, Fluka) as supporting electrolyte. Concentrations of the Cu(II) complexes were about 10^{-4} M. A three-electrode setup was used with a glassy carbon working electrode, a coiled platinum wire as counter electrode, and a coiled silver wire as a pseudoreference electrode. Cobaltocenium hexafluorophosphate was used as internal reference. In a separate experiment the potential difference between the cobaltocenium/cobaltocene and ferrocene/ferrocenium (FcH/FcH^+) redox couples was determined. All values are referenced to the FcH/FcH^+ redox couple. The scan rate was 100 mV/s.

2.7. In situ preparation of Cu(II) complex solutions

For the experiments described in the following Cu(II) complex solutions (**1**Cl_2, **2**Cl_2 and **3**Cl_2) were prepared *in situ* as follows: 500 µL of a 2 mM ligand solution in DMSO and 500 µL of a 0.8 mM $CuCl_2$ aqueous solution were combined resulting in 1 mL of a 0.4 mM complex solution (Cu(II):ligand = 1:2.5, water:DMSO = 1:1).[1]

2.8. DNA cleavage studies

Plasmid DNA pBR322 was purchased from Carl Roth. All DNA cleavage experiments were performed in triplicate in order to ensure reproducibility. The standard deviation was used to calculate the error bars.

The complexes and their corresponding ligands (100 µM $CuCl_2$/250 µM ligand from the above described solution or 250 µM ligand only) were incubated with plasmid DNA pBR322 (0.025 mg/mL) buffered in MOPS (50 mM, pH 7.4) in the absence and the presence of ascorbic acid or glutathione (1 mM) as reducing agent, respectively, for 2 h at 37 °C. Gel electrophoresis was carried out for 2 h at 40 V using a 1% agarose gel in 0.5× TBE (Tris/Borate/EDTA) buffer containing ethidium bromide (0.2 µg/mL). The bands of supercoiled (S), open-circular/nicked (N), and linear (L) DNA were visualized by fluorescence imaging of intercalating ethidium bromide on a Bio-Rad GelDoc EZ Imager. Data analysis was performed with Bio-Rad's Image Lab Software (Version 3.0). Due to the decreased affinity of ethidium

[1] For CD spectroscopy, the final Cu(II):ligand ratio was 1:2.

bromide to supercoiled DNA a correction factor of 1.22 was used [29].

2.9. Detection of ROS

For the determination of ROS generated by *in situ* prepared Cu(II) complex **2**Cl_2 the general DNA cleaving procedure as described above was applied in the presence of ascorbate (1 mM) and one of the following ROS scavengers: DMSO (400 mM), NaN_3 (10 mM), pyruvic acid (2.5 mM) or superoxide dismutase (625 U/mL). In the case of pyruvate as a ROS scavenger a MOPS buffer concentration of 75 mM was needed to keep the pH value constant at 7.4.

2.10. Melting point determination

Melting curves of calf thymus DNA (CT-DNA, 50 μM) in MOPS buffer (50 mM, pH 7.4) in the presence of the *in situ* prepared Cu(II) complexes **1**Cl_2, **2**Cl_2 and **3**Cl_2 (2.5 μM) and their corresponding ligands (6.25 μM) were measured on a Varian Cary 100 Bio UV–VIS spectrophotometer at 260 nm using a heating rate of 0.5 °C/min. Four Hellma cuvettes with 1 mL sample volume each were used for carrying out the experiment simultaneously. Normalization of melting curves was utilized for better visualization.

2.11. Ethidium bromide (EtBr) displacement assay

For recording the fluorescence emission spectra of ethidium bromide intercalated into DNA a Varian Cary Eclipse fluorescence spectrophotometer was used. A mixture of CT-DNA (20 μM) and EtBr (1.3 μM) in MOPS buffer (50 mM, pH 7.4) was prepared in a 1 mL fluorescence cuvette. After 15 min, this solution was treated with increasing amounts of the *in situ* prepared Cu(II) complex (**1**Cl_2, **2**Cl_2 and **3**Cl_2) or the corresponding ligand. The fluorescence spectra were collected after each addition in a range of 550–700 nm using an excitation wavelength of 518 nm (photomultiplier voltage: 1000 V).

2.12. Circular dichroism (CD) spectroscopy

CD spectra of CT-DNA (100 μM) in MOPS buffer (50 mM, pH 7.4) were recorded on a Jasco J-810 spectrometer in a range of 220 to 320 nm with a measuring velocity of 100 nm/min and a data point interval of 0.1 nm. *In situ* prepared Cu(II) complexes **1**Cl_2, **2**Cl_2 and **3**Cl_2 and their corresponding ligands were added stepwise (5 μM $CuCl_2$/10 μM ligand to 20 μM $CuCl_2$/40 μM ligand for the complexes and 10 μM to 40 μM for the ligand) to investigate their mode of interaction towards DNA. The volume of all samples was adjusted to 1 mL. All samples contained 10% DMSO.

3. Results and discussion

3.1. Synthesis of Cu(II) complexes

The ligands bimzS, bimzE and bimzB, were synthesized according to the literature [23,25–28]. The synthesis of the Cu(II) complexes [Cu(bimzE)$_2$](ClO_4)$_2$ (**2**(ClO_4)$_2$) and [Cu(bimzB)$_2$](NO_3)$_2$ (**3**(NO_3)$_2$) is also described in the literature, which is the reason why these particular counter ions were used [23,24].

When the synthetic procedure for Cu(II) complexes **2**(ClO_4)$_2$ and **3**(NO_3)$_2$ was applied to **1**(NO_3)$_2$, a decomposition of the ligand bimzS (disulfide bridge) was observed in the ESI mass spectra as indicated by peaks representing free benzimidazole and a Cu(I) species coordinated by two benzimidazole moieties (Fig. S3b and c). Based on literature reports for the reaction of Cu(I) with 2-mercaptobenzimidazole we assume a decomposition of bimzS to free benzimidazole *via* reduction, oxidation and hydrolysis steps (Scheme 1) [30]. X-ray crystallography on a solid obtained from the reaction solution as described above but in DMF as a solvent, showed the same composition of the resulting Cu(II) species as in [30].[2] Based on UV–VIS spectroscopic, mass spectrometric (*vide infra*) and X-ray crystallographic results we assume, that in the synthesis solution for **1**(NO_3)$_2$ a mixture of **1**(NO_3)$_2$ and [Cu(benzimidazole)$_4$]$^{2+}$ is present.

Although elemental analysis indicated the formation of Cu(II) complexes, ESI-MS data showed the presence of Cu(I) in case of **1**(NO_3)$_2$ and **2**(ClO_4)$_2$. Such a reduction during the ESI-MS measurement can be ascribed to MeCN dilution of the corresponding complex solutions [31,32]. The tendency for reduction can be explained by the difference in the two ligand systems: bimzS and bimzE represent flexible ligands and bimzB a rather stiff ligand regarding the linkage of the two benzimidazole moieties. Thus, bimzB with a twisted V-shaped form is able to stabilize a square-planar Cu(II) complex, but not a tetrahedral Cu(I) complex, excluding such a Cu(II) reduction effect during MS measurement for **3**(NO_3)$_2$ [23]. The more flexible ligand bimzE provides a square-planar N_4 system for the Cu(II) complex **2**(ClO_4)$_2$, which is more distorted when compared to **3**(NO_3)$_2$ [24]. The same can be assumed for the flexible ligand in **1**(NO_3)$_2$, which is thus prone to reduction.

3.2. UV–VIS spectroscopy

UV–VIS data indicated the formation of a Cu(I) species in the reaction mixture for **1**(NO_3)$_2$ directly after refluxing, which is transformed slowly into Cu(II) within two days. This is suggested by an increase of the d→d transition band appearing at around 688 nm (Table 1, Fig. S4a). The bands in the region 220–280 nm (π→π* transition) are unaffected during this time period, as expected. We assume that a mixture of a tetra(benzimidazole) complex species and **1**(NO_3)$_2$ is present directly after synthesis due to disulfide decomposition (Scheme 1). This is suggested by comparison of UV–VIS data in the region of 200–400 nm (π→π* transitions) for the reaction mixture **1**(NO_3)$_2$, *in situ* prepared **1**(NO_3)$_2$ and *in situ* prepared [Cu(benzimidazole)$_4$](NO_3)$_2$ (Table 1, Fig. S4b).

3.3. EPR spectroscopy

UV–VIS spectroscopy indicated that a Cu(I) species is present in the reaction mixture of **1**(NO_3)$_2$ directly after synthesis, supposedly [Cu(benzimidazole)$_4$]$^+$. In order to prove this, and oxidation to a Cu(II) species (assumedly [Cu(benzimidazole)$_4$]$^{2+}$) within two days due to oxidation by atmospheric oxygen, EPR spectroscopy was applied. In Fig. 2 the EPR spectra of the reaction mixture of **1**(NO_3)$_2$ by following the general synthetic procedure for the Cu(II) complexes is shown directly after synthesis and after one and two days, respectively. In order to obtain quantitative data, the parameters used for the EPR measurements, and the concentration of the samples used, were identical for all cases.

As expected the characteristic signal for Cu(II) increased during 48 h and shows typical g_{II} and $g_{\perp}$ values with the corresponding hyperfine coupling A_{II} for a square planar geometry of a CuN_4 system with a d_{x2-y2} ground state [33,34]. Furthermore, EPR spectroscopy was carried out for the Cu(II) complexes **2**(ClO_4)$_2$ (Fig. S5a) and **3**(NO_3)$_2$ (Fig. S5b) under the same conditions. All data at room temperature and at 163 K are listed in Table 2.

As all the data are in the same range, it can be assumed that the square planar CuN_4 system in the Cu(II) complexes **2**(ClO_4)$_2$ and **3**(NO_3)$_2$ [23,24] is in the d_{x2-y2} ground state [33]. Additionally, the observed values are comparable to literature known Cu(II) complexes with similar ligands [23,34–36]. In these cases, an increase of g_{II} and a decrease of A_{II} is associated with an enhancement of a tetrahedral distortion of square planar Cu(II) complexes [24,34]. Although g_{II} is

[2] The quality of the crystallographic data set was not good enough and is thus not presented here.

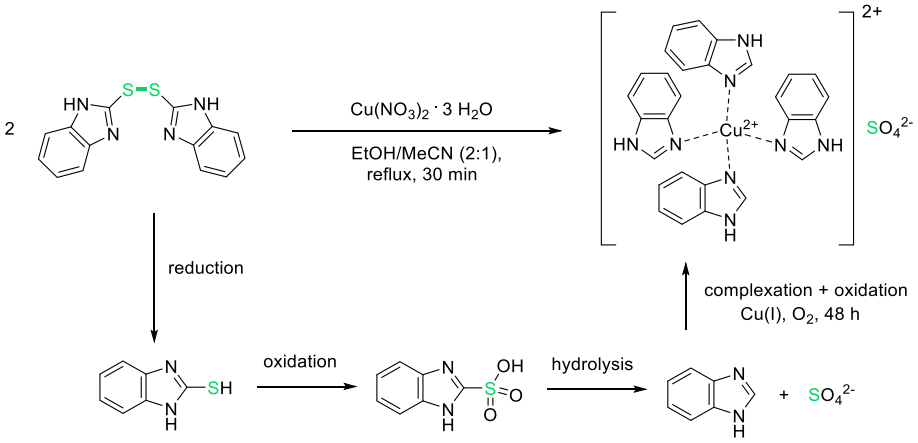

Scheme 1. Proposed decomposition of the disulfide bridge of bimzS in the synthesis of **1**$(NO_3)_2$.

Table 1
UV–VIS data of the reaction mixtures of **1**$(NO_3)_2$, **2**$(ClO_4)_2$ and **3**$(NO_3)_2$ (10 mM/0.08 mM in EtOH:MeCN = 2:1 for d➔d transitions/π➔π* transitions, for **2**$(ClO_4)_2$ and **3**$(NO_3)_2$ including also 50 mM MOPS pH 7.4) and for comparison *in situ* prepared **1**$(NO_3)_2$ and [Cu(benzimidazole)$_4$]$(NO_3)_2$ (1 mM/0.05 mM in EtOH:MeCN = 2:1 for d➔d transitions/π➔π* transitions).

Reaction mixture/assumed species	Day	Color	Absorption maxima (nm)
1$(NO_3)_2$ & [Cu(benzimidazole)$_4$]NO_3	0	Orange	226, 267, 272, 280, 295, 307
1$(NO_3)_2$ & [Cu(benzimidazole)$_4$]$(NO_3)_2$	1	Yellow-green	225, 267, 274, 280, 295, 308, 688
1$(NO_3)_2$ & [Cu(benzimidazole)$_4$]$(NO_3)_2$	2	Green	224, 268, 274, 279, 294, 688
2$(ClO_4)_2$ [a]	0	Dark-green	233, 242, 274, 281, 580, 681
3$(NO_3)_2$ [b]	0	Blue	231, 278, 285, 580
In situ prepared Cu(II) complexes			
1$(NO_3)_2$	0	Orange	212, 225, 250, 268, 275, 285, 296, 306
[Cu(benzimidazole)$_4$]$(NO_3)_2$	0	Blue	212, 244, 250, 273, 279, 680

[a] Literature values for **2**$(ClO_4)_2$ (solvent unknown) [24]: 370 nm (LMCT), 510, 641 nm (d➔d transitions).
[b] Literature values for **3**$(NO_3)_2$ in EtOH [23]: 224, 280 nm (π➔π* transition), 390 nm (n➔π* transition).

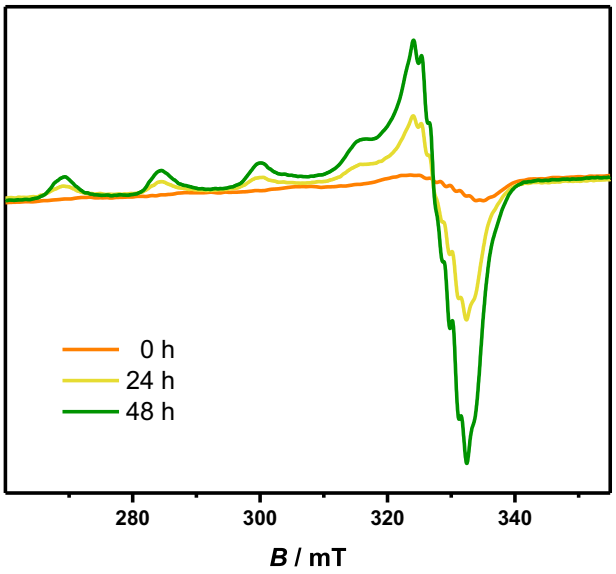

Fig. 2. EPR spectra of the reaction mixture of **1**$(NO_3)_2$ in EtOH/MeCN (2:1) directly after synthesis and after 24 and 48 h, respectively, at 163 K (frozen solution) and 9.5 GHz (X-band frequency).

unchanged when **2**$(ClO_4)_2$ is compared with **3**$(NO_3)_2$, the significant decrease in A_{II} indicates that the square planar complex **2**$(ClO_4)_2$ is more tetrahedrally distorted than **3**$(NO_3)_2$. This may be due to the more flexible ethylene bridge in comparison to the rigid *ortho*-phenylene bridge. Additionally, the molecular structure in the solid state of **3**$(NO_3)_2$ displayed an ideal square planar geometry in the CuN_4 system whereas in **2**$(ClO_4)_2$ a square planar structure with significant tetrahedral distortion is present [23,24]. This occurrence is in accordance with the EPR data in this work.

3.4. Cyclic voltammetry

In order to investigate the reduction processes of the reaction mixtures of **1**$(NO_3)_2$, **2**$(ClO_4)_2$ and **3**$(NO_3)_2$ cyclic voltammetry was carried out to obtain the half-wave potential $E_{1/2}$ of the Cu(II)/Cu(I) cycle. In Fig. 3 the cyclic voltammograms for Cu(II) complexes **2**$(ClO_4)_2$ and **3**$(NO_3)_2$ with a scan rate of 100 mV/s are shown (for scan rate dependence see Fig. S6). However, the cyclic voltammogram of the reaction mixture of **1**$(NO_3)_2$ displayed too many undefined peaks. This is probably due to the disulfide bridge being also involved in redox chemistry or decomposition of bimzS to the free benzimidazole.

The cyclic voltammograms deliver the $E_{1/2}$ of the Cu(II)/Cu(I) reduction *vs.* FcH/FcH^+, which are listed in Table 3. The calculation of the rate of heterogeneous electron transfer indicates a quasi-reversible redox process for both **2**$(ClO_4)_2$ and **3**$(NO_3)_2$ (*cf.* S6).

The results suggest that the more flexible the bridge between the connected benzimidazole moieties the more favorable the geometrical switch (square planar/tetrahedral), which results in an easier Cu(II) reduction and reoxidation. Thus, the redox potential of **2**$(ClO_4)_2$ is much higher than that of **3**$(NO_3)_2$ and should generate ROS in a higher extent, a feature that was investigated in further DNA cleavage studies.

3.5. DNA cleavage studies

The DNA cleavage can follow either an oxidative cleavage or a hydrolytic cleavage pathway [19]. For most Cu(II) complexes, which cleave DNA in an oxidative manner, an external reducing agent like

Table 2
EPR data of the Cu(II) complex solutions of **1**$(NO_3)_2$ (after 48 h), **2**$(ClO_4)_2$ and **3**$(NO_3)_2$.

Reaction mixture/assumed species	g_{iso} value at 298 K	g values and hyperfine coupling constant A_{II} at 163 K
1$(NO_3)_2$ & [Cu(benzimidazole)$_4$]$(NO_3)_2$	2.113	$g_{\|\|}$ = 2.313; $g_{\perp}$ = 2.064; A_{II} = 15.1 mT
2$(ClO_4)_2$	2.125	$g_{\|\|}$ = 2.309; $g_{\perp}$ = 2.080; A_{II} = 14.4 mT
3$(NO_3)_2$	2.095	$g_{\|\|}$ = 2.310; $g_{\perp}$ = 2.071; A_{II} = 15.5 mT

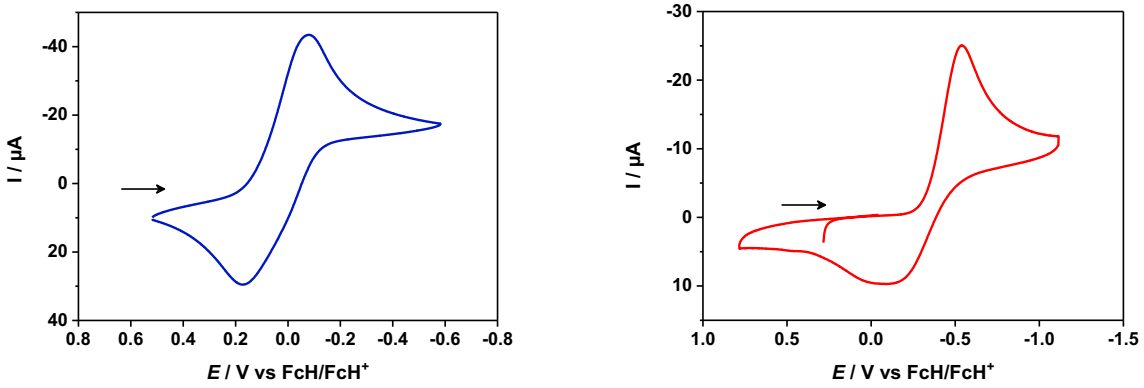

Fig. 3. Cyclic voltammograms for the reduction processes of Cu(II) complexes **2**$(ClO_4)_2$ (left) and **3**$(NO_3)_2$ (right) in EtOH/MeCN (2:1) with 0.1 M NBu_4PF_6 as supporting electrolyte. The scan rate was 100 mV/s.

Table 3
CV data of **2**$(ClO_4)_2$ and **3**$(NO_3)_2$.

Cu(II) complex	$E_{1/2}$ [V] of Cu(II)/Cu(I) reduction *vs.* FcH/FcH$^+$
2$(ClO_4)_2$ (flexible ethylene bridge)	+0.05
3$(NO_3)_2$ (rigid *ortho*-phenylene bridge)	−0.31

ascorbate is needed to generate Cu(I), thus initiating a Cu(II)/Cu(I) redox cycle and consequently the generation of reactive oxygen species (Scheme 2) [37].

Indeed, an increased generation of ROS should be the consequence of a fast and easy Cu(II)/Cu(I) redox cycling. Thus, we expect for the Cu (II) species **2** with the flexible ethylene bridge a more efficient ROS generation and therefore a better nuclease activity than for the Cu(II) species **3** with the rigid *ortho*-phenylene bridge.

3.5.1. Oxidative cleavage

In order to investigate the oxidative cleavage activity of the Cu(II) species $[Cu(bimzS)_2]^{2+}$ (**1**), $[Cu(bimzE)_2]^{2+}$ (**2**) and $[Cu(bimzB)_2]^{2+}$ (**3**) and their ligands bimzS, bimzE and bimzB, their ability to convert supercoiled (S) plasmid DNA pBR322 into open-circular/nicked (N) and linear (L) DNA forms, respectively, was evaluated using agarose gel electrophoresis. DNA was incubated with the corresponding *in situ* prepared Cu(II) complexes (100 µM) or ligands (250 µM) for 2 h at 37 °C in the presence or absence of the reducing agent ascorbate or glutathione. The pH value was kept constant at 7.4 using MOPS buffer instead of the commonly used Tris buffer in order to avoid potential competitive coordination of the buffer to Cu(II) [38]. Furthermore due to the insufficient solubility of the ligands in common solvents and in order to prevent precipitation of the ligand during incubation the complex solution was prepared *in situ* in a Cu(II):ligand ratio of 1:2.5 using $CuCl_2$ as a Cu(II) source.[3] An excess of ligand was used to avoid

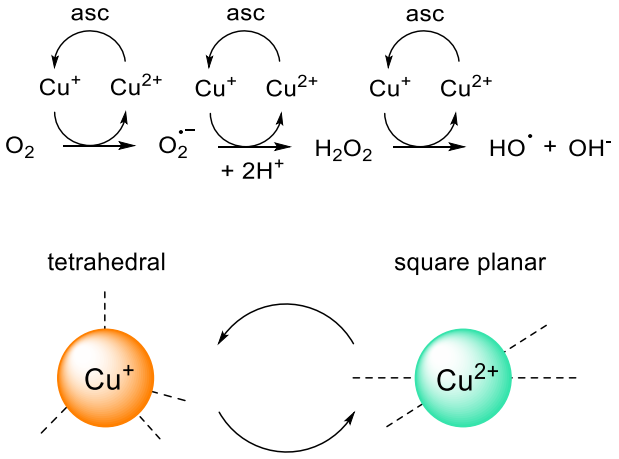

Scheme 2. (Above) Generation of reactive oxygen species (ROS) by a Cu(II)/Cu (I) redox cycle in the presence of ascorbate (asc) as reducing agent [37]. (Below) Visualization of the geometrical change between Cu(II) (square planar) and Cu(I) (tetrahedral) complexes within the redox cycle.

free Cu(II). For the replacement of ClO_4^- and NO_3^- counterions, respectively, by Cl^- ions, no influence on the nuclease activity is to be expected [39].

In order to prove that the Cu(II) complexes prepared *in situ* (**1**Cl_2, **2**Cl_2 and **3**Cl_2) are indeed responsible for DNA binding and cleavage, mass spectrometry measurements were carried out with *in situ* prepared complex solutions **1**Cl_2, **2**Cl_2 and **3**Cl_2 similar to the conditions during incubation with DNA (Cu(II):ligand = 1:2.5, water:DMSO = 1:1, incubation for 2 h at pH 7.4 and 37 °C (Fig. S7a–c)). The observed masses indeed matched with those of the Cu(II) complexes shown in Fig. 1. For **1**Cl_2 and **2**Cl_2, the formation of reduced Cu(I) species can be ascribed to

[3] In order to ensure comparability a common counter ion was chosen, whereas for the synthesis either ClO_4^- or NO_3^- had to be used. No precipitation of the ligand or complex was observed in the incubated 0.4 mM complex stock solutions (in contrast to the synthetic procedure with a complex concentration about 10 mM). Accordingly, no precipitation is expected during DNA cleavage experiments (complex concentration 100 µM).

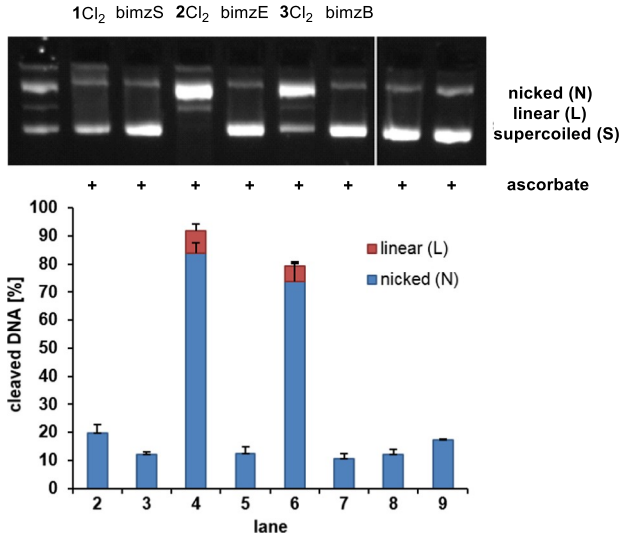

Fig. 4. (Above) Cleavage of plasmid DNA pBR322 (0.2 µg) by complexes **1**Cl_2, **2**Cl_2 and **3**Cl_2 and their corresponding ligands in MOPS buffer (50 mM, pH 7.4) after incubation for 2 h at 37 °C in the presence of ascorbate (1 mM). Lane 1: DNA ladder (S/N/L), lane 2: **1**Cl_2 (100 µM), lane 3: bimzS (250 µM), lane 4: **2**Cl_2 (100 µM), lane 5: bimzE (250 µM), lane 6: **3**Cl_2 (100 µM), lane 7: bimzB (250 µM), lane 8: DNA reference (12.5% DMSO), lane 9: DNA reference without DMSO. (Below) Visualization of the cleaved DNA in percentage.

MeCN dilution of the samples for the MS measurement (*vide supra*).

The nuclease activity of *in situ* prepared Cu(II) complexes **1**Cl_2, **2**Cl_2 and **3**Cl_2 and the ligands bimzS, bimzE and bimzB in the presence of ascorbate (1 mM) is shown in Fig. 4. Since the ligands themselves do not show any effect, an excess of them in the incubation mixture (1:2.5 instead of the expected stoichiometry 1:2) should not pose any problems within these experiments. Complex **1**Cl_2 did not show any cleavage activity. It is probably inactive due to the consumption of reducing agents for the reduction of the disulfide bond [40].

The ligands bimzS, bimzE and bimsB and their corresponding complexes do not show any cleavage activity in the absence of a reducing agent (Fig. S8). In contrast to the inactive complex **1**Cl_2, complexes **2**Cl_2 and **3**Cl_2 efficiently cleave supercoiled plasmid DNA into linear DNA at a concentration of 100 µM, only in the presence of ascorbate as a reducing agent (Fig. 4). These DNA cleavage activities are in the same order of magnitude as for other Cu(II) complexes with benzimidazole ligands under comparable incubation conditions [20,21,41,42–45]. The nuclease activity of **2**Cl_2 is significantly higher than that of **3**Cl_2. As noted before, the tetrahedral Cu(I) species is preferred in **2**Cl_2 than in **3**Cl_2. This is caused by the more flexible ligand bimzE in **2**Cl_2 [23,24], supporting a fast redox cycle Cu(II)/Cu(I) and thus oxidative cleavage activity.

In the presence of the reducing agent glutathione (1 mM), no nuclease activity is observed for **1**Cl_2, **2**Cl_2 and **3**Cl_2 (Fig. S9). We suggest that the higher standard redox potential at pH 7 of glutathione (−0.17 V) in comparison to ascorbate (−0.34 V) does not allow the start the catalytic cycle with the redox couple Cu(II)/Cu(I) of the complexes for generation of ROS [46,47].

3.5.2. Reactive oxygen species (ROS)

In order to confirm redox chemistry comprising ROS formation as a cleavage mechanism, quenching experiments were carried out. Representatively, *in situ* prepared Cu(II) complex **2**Cl_2 (100 µM) was incubated with plasmid DNA pBR322 in the presence of ascorbate (1 mM) for 2 h at 37 °C with certain ROS scavengers. In Table 4, ROS scavengers are listed with the corresponding reactive species [48–51]. In Fig. 5 the nuclease activity of **2**Cl_2 in the absence and presence of the corresponding ROS quenchers is shown.

Table 4
ROS and their quenchers.

Scavenger	ROS
DMSO	Hydroxyl radicals (·OH) [48]
NaN_3	Singlet oxygen ($^1O_2$) [49]
Pyruvate	Hydrogen peroxide (H_2O_2) [50]
Superoxide dismutase (SOD)	Superoxide anion radicals ($\cdot O_2^-$) [51]

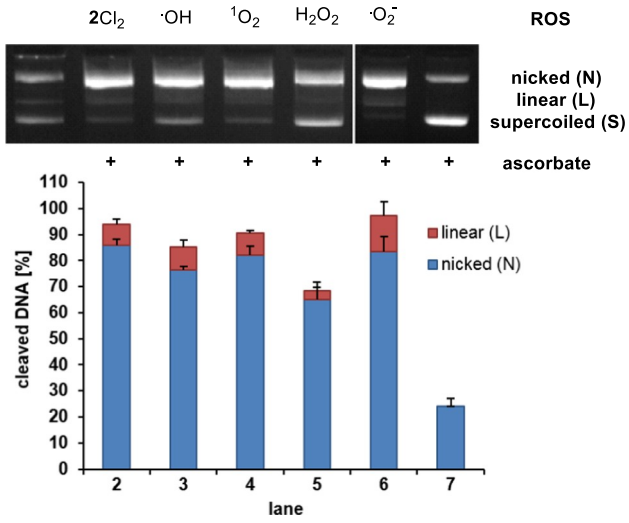

Fig. 5. (Above) Cleavage of plasmid DNA pBR322 (0.2 µg) by **2**Cl_2 (100 µM) in MOPS buffer (50 mM, pH 7.4) with ascorbate (1 mM) after incubation for 2 h at 37 °C in the absence and presence of corresponding ROS scavengers. Lane 1: DNA ladder (S/N/L), lane 2: **2**Cl_2, lane 3: **2**Cl_2 + DMSO (400 mM), lane 4: **2**Cl_2 + NaN_3 (10 mM), lane 5: **2**Cl_2 + pyruvate (2.5 mM), lane 6: **2**Cl_2 + SOD (625 u/mL), lane 7: DNA reference (12.5% DMSO). (Below) Visualization of the cleaved DNA in percentage.

Compared to the nuclease activity of **2**Cl_2 without any ROS scavenger (lane 2), the DNA cleavage activity of **2**Cl_2 is decreased slightly in the presence of DMSO (lane 3) and significantly in the presence of pyruvate (lane 5) indicating the occurrence of hydroxyl radicals (·OH) and hydrogen peroxide (H_2O_2) and thus proving an oxidative DNA cleavage pathway. It has to be mentioned that all samples contained 12.5% DMSO (1.75 M), a solvent used here due to its hydroxyl radical quenching activity, however, at only 400 mM concentration. Also, the quenching experiment shows that the occurrence of single oxygen ($^1O_2$) and superoxide anion radicals ($\cdot O_2^-$) precluded during incubation due to equal nuclease activity in the presence and absence of the corresponding scavenger.

3.6. DNA binding studies

3.6.1. Melting point determination

In order to evaluate the binding of the *in situ* prepared Cu(II) complexes **1**Cl_2, **2**Cl_2 and **3**Cl_2 and their corresponding ligands bimzS, bimzE and bimzB to DNA, their influence on the DNA melting temperature T_m due to stabilization of the double helix was investigated. The magnitude of increasing the thermal denaturation temperature gives an insight into the strength of DNA binding. The melting temperature is the point where half of the double helix DNA strand has changed over to the single stranded DNA. This can be monitored by UV–VIS spectroscopy due to different absorption coefficients of both DNA forms [52].

For the melting studies *in situ* prepared Cu(II) complexes **1**Cl_2, **2**Cl_2 and **3**Cl_2 (2.5 µM) or the corresponding ligands (6.25 µM) were mixed with CT-DNA (50 µM) in MOPS buffer (50 mM, 7.4) and heated up slowly from 65 to 90 °C. All samples contained 1.25% DMSO including

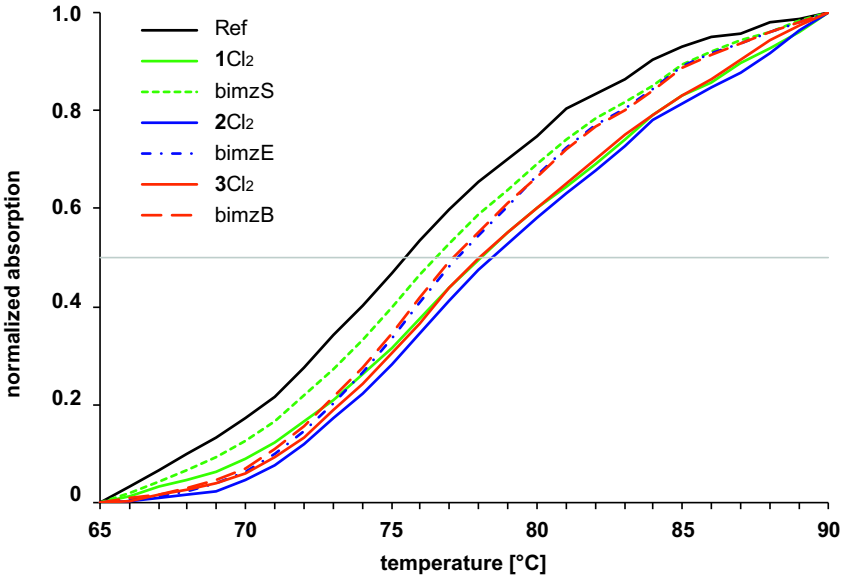

Fig. 6. Normalized CT-DNA melting curves in the absence (Ref) and presence of complexes $\mathbf{1}Cl_2$, $\mathbf{2}Cl_2$ and $\mathbf{3}Cl_2$ and their corresponding ligands bimzS, bimzE and bimzB.

Table 5
Thermal denaturation temperature T_m of Cu(II) complexes $\mathbf{1}Cl_2$, $\mathbf{2}Cl_2$ and $\mathbf{3}Cl_2$ and their ligands and temperature difference ΔT_m related to T_m of CT-DNA.

Compound	T_m [°C]	ΔT_m [°C]
CT-DNA (ref)	75.5	0
$\mathbf{1}Cl_2$	78.1	2.6
bimzB	76.6	1.1
$\mathbf{2}Cl_2$	78.5	3.0
bimzE	77.3	1.8
$\mathbf{3}Cl_2$	78.1	2.6
bimzB	77.2	1.7

the reference. The visualization of melting curves after normalization is shown in Fig. 6 and the melting points of CT-DNA in the presence of complexes and ligands are listed in Table 5.

Complexes $\mathbf{1}Cl_2$, $\mathbf{2}Cl_2$ and $\mathbf{3}Cl_2$ exhibited a higher binding affinity to CT-DNA than the ligands bimzS, bimzE and bimzB. The positively charged Cu(II) complexes might possess a higher affinity for the negatively charged phosphate backbone of the DNA in comparison to the neutral ligands. Furthermore, for $\mathbf{2}Cl_2$ with the more flexible ligand we observed the highest ΔT_m value (3.0 °C) compared to both $\mathbf{1}Cl_2$ and $\mathbf{3}Cl_2$ (2.6 °C). All values indicate groove binding and/or electrostatic interaction as possible DNA binding mode [53]. Although all ΔT_m for the complexes are in the same range, the differences in oxidative nuclease activity are more pronounced (*vide supra*, $\mathbf{2}Cl_2 > \mathbf{3}Cl_2 \gg \mathbf{1}Cl_2$). This indicates the importance of the redox properties in contrast to the actual strength of DNA binding.

3.6.2. EtBr displacement assay

Another method to investigate the binding of the *in situ* prepared Cu(II) complexes $\mathbf{1}Cl_2$, $\mathbf{1}Cl_2$ and $\mathbf{3}Cl_2$ and their corresponding ligands bimzS, bimzE and bimzB towards CT-DNA is the EtBr displacement assay. In the presence of DNA EtBr emits enhanced and intense fluorescence, due to intercalation of EtBr between the base pairs of the DNA. In presence of competitive DNA binding molecules like the Cu(II) complexes $\mathbf{1}Cl_2$, $\mathbf{2}Cl_2$ and$\mathbf{3}Cl_2$, EtBr can be displaced causing a decreased fluorescence emission [54]. The magnitude of decrease of the fluorescence emission of EtBr by displacement with a competitive compound, gives an insight into its DNA binding ability. The classical Stern-Volmer equation [55], which can be applied here, is

$$\frac{I_0}{I} = 1 + K_{SV}[Q] \quad (1)$$

where I_0 is the fluorescence emission in absence and I in presence of a competitive molecule, and [Q] is the concentration of the competitor. Titration of a competitive quencher yields the Stern-Volmer constant K_{SV} by plotting its concentration [Q] against I_0/I. In order to obtain the binding constant K_{app} towards DNA of the Cu(II) complexes $\mathbf{1}Cl_2$, $\mathbf{2}Cl_2$ and $\mathbf{3}Cl_2$ and their ligands the equation

$$K_{EtBr}[EtBr] = K_{app}[Q] \quad (2)$$

is used, where K_{EtBr} is the binding constant of EtBr towards DNA ($10^7\,M^{-1}$) [56] and *[EtBr]* is the concentration of EtBr (1.3 μM). *[Q]* is the concentration of the competitor, where the fluorescence emission of EtBr is quenched by 50%, which can be calculated by using Eq. (1).

A visualization of a fluorescence emission quenching experiment by titration of the *in situ* prepared Cu(II) complexes $\mathbf{2}Cl_2$ and $\mathbf{3}Cl_2$, respectively, to a DNA-EtBr starting system (I_0) is given in Figs. 7 and 8. All calculated K_{SV} and K_{app} values are listed in Table 6. EtBr displacement titrations and the corresponding plots for calculation of K_{SV} for $\mathbf{1}Cl_2$ and all ligands can be found in the supporting information (Fig. S10a–d).

For the DNA binding studies of the *in situ* prepared Cu(II) complexes $\mathbf{1}Cl_2$, $\mathbf{2}Cl_2$ and $\mathbf{3}Cl_2$ and their ligands the same trends were observed in the EtBr displacement assay as in the melting point determination, which shows the compatibility of both methods. All ligands showed a similar but decreased binding affinity to DNA in comparison to their Cu(II) complexes. The higher binding constants of the complexes might be attributed to additional electrostatic effects. However, also quenching of EtBr fluorescence by the paramagnetic Cu(II) ions is conceivable [57]. In accordance with DNA melting studies, all Cu(II) complexes exhibit K_{app} values in a range, which suggests groove binding and/or electrostatic interaction as the mode of DNA binding [53,58].

By comparing complexes $\mathbf{1}Cl_2$, $\mathbf{2}Cl_2$ and $\mathbf{3}Cl_2$ there is an excellent correlation with the DNA cleavage experiments. The Cu(II) complex $\mathbf{2}Cl_2$ with the highest nuclease activity shows a three times higher binding affinity than $\mathbf{1}Cl_2$ and $\mathbf{3}Cl_2$, which results in a better nuclease activity. Although we consider an appropriate redox potential as a very important factor for the high DNA cleavage activity of $\mathbf{2}Cl_2$ (*vide supra*), its higher DNA affinity due to its more flexible ligand in comparison to $\mathbf{1}Cl_2$ and $\mathbf{3}Cl_2$ might also play a role in this regard. Complex $\mathbf{3}Cl_2$

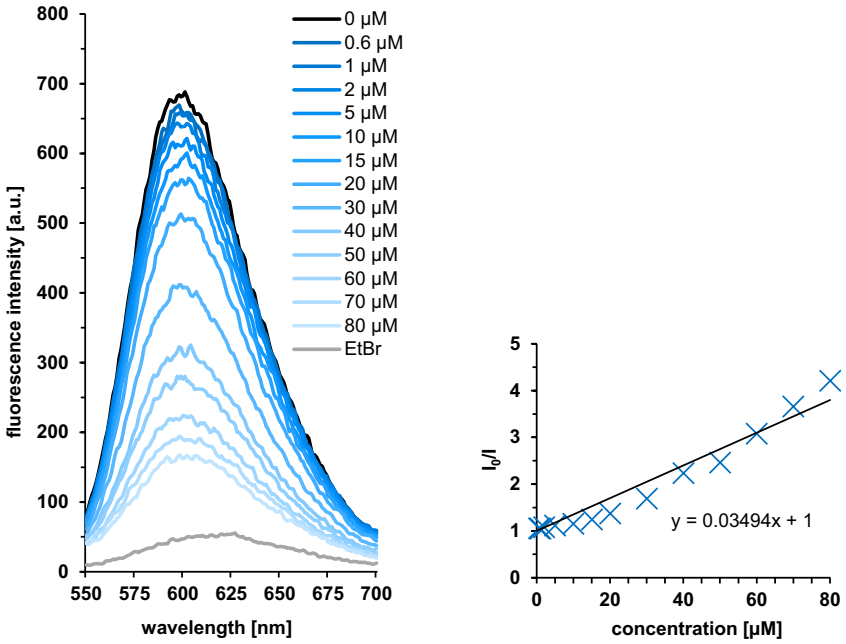

Fig. 7. (Left) EtBr displacement of the EtBr-CT-DNA system (1.3 µM EtBr, 20 µM CT-DNA) in MOPS buffer (50 mM, pH 7.4) by titration of the Cu(II) complex **2**Cl_2. (Right) I_0/I over *[Q]* to calculate K_{SV}.

exhibiting a similar K_{app} value like complex **1**Cl_2 might still show higher DNA cleavage activity in comparison to **1**Cl_2 due to its favorable redox characteristics.

3.6.3. CD spectroscopy

CD spectroscopy is a commonly used optical technique to investigate the mode of DNA interaction (intercalation, groove binding) of metal complexes towards DNA. In general, CD spectra of CT-DNA represent a negative band at 245 nm due to the helicity of the B-form of DNA and a positive band at 275 nm caused by base-stacking of the nucleobases [59]. A shift (both increase or decrease) of the positive band indicates intercalation of metal complexes, whereas a decrease of

Table 6
Stern-Volmer constants K_{SV} and binding constants K_{app} towards CT-DNA for the Cu(II) complexes **1**Cl_2, **2**Cl_2 and **3**Cl_2 and their corresponding ligands.

Compound	K_{SV} [M^{-1}]	K_{app} [M^{-1}]
1Cl_2	1.04×10^4	1.35×10^5
bimzS	2.48×10^3	3.22×10^4
2Cl_2	3.49×10^4	4.54×10^5
bimzE	2.40×10^3	3.12×10^4
3Cl_2	9.97×10^3	1.30×10^5
bimzB	1.67×10^3	2.17×10^4

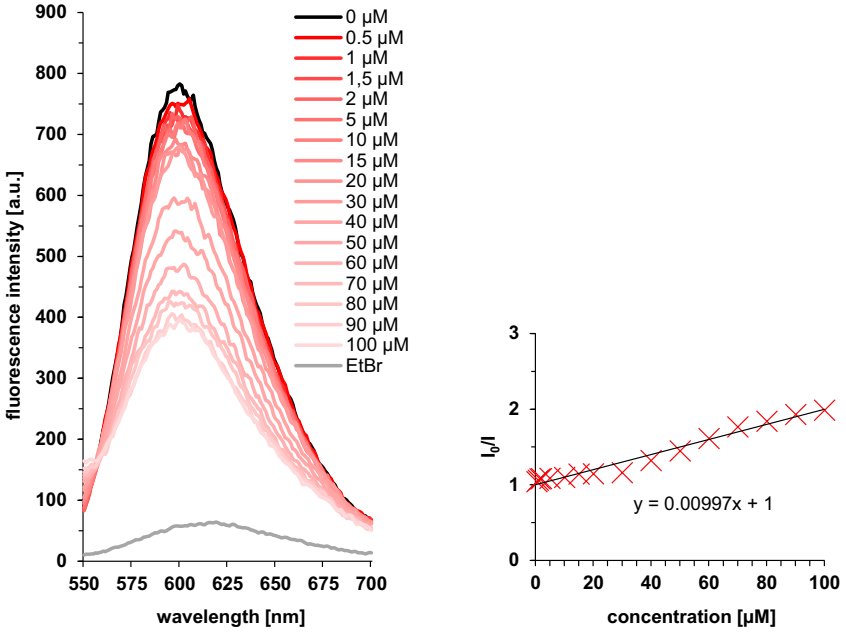

Fig. 8. (Left) EtBr displacement of the EtBr-CT-DNA system (1.3 µM EtBr, 20 µM CT-DNA) in MOPS buffer (50 mM, pH 7.4) by titration of the Cu(II) complex **3**Cl_2. (Right) I_0/I over *[Q]* to calculate K_{SV}.

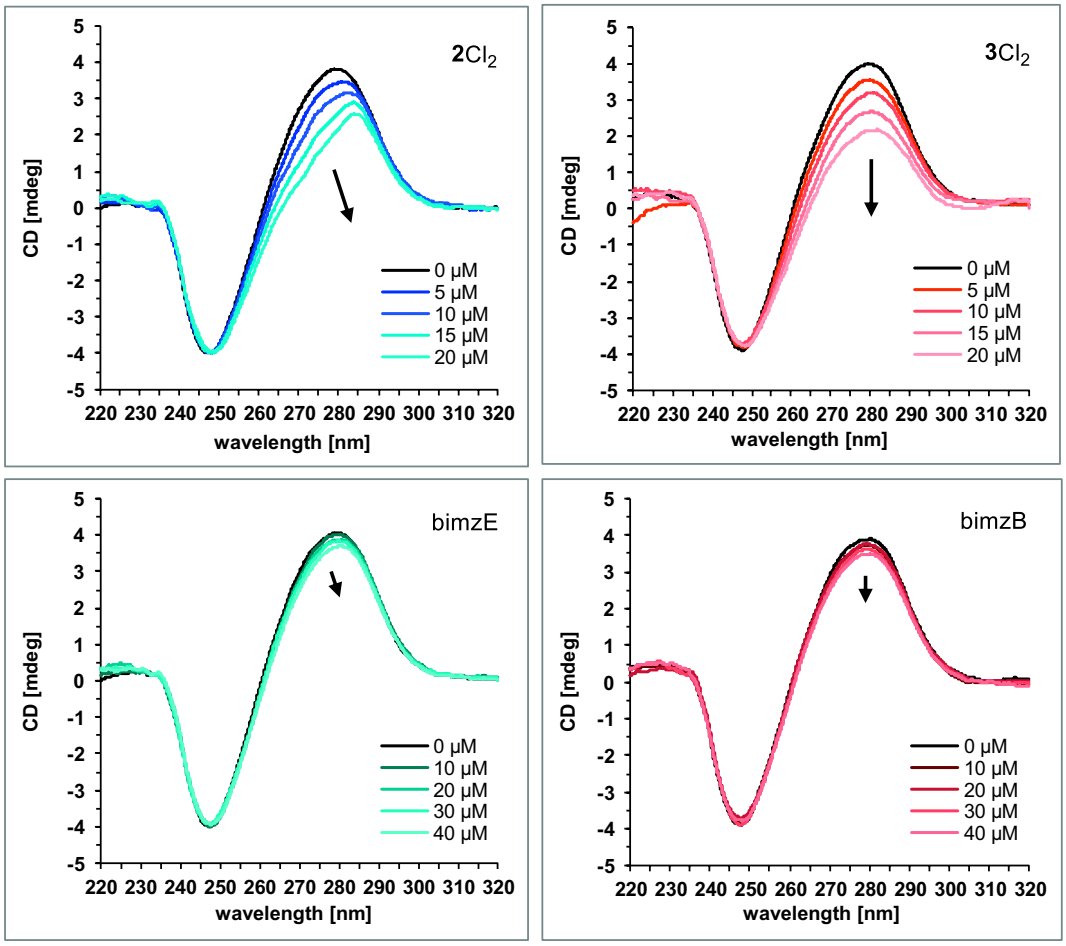

Fig. 9. CD spectra of CT-DNA (100 µM) in MOPS buffer (50 mM, pH 7.4) with increasing concentrations of $\mathbf{2}Cl_2$ and $\mathbf{3}Cl_2$ (0–20 µM) (above) and their corresponding ligands bimzE and bimzB (0–40 µM) (below). All samples contained 10% DMSO.

the negative band hints at groove binding interaction [60–62]. The CD spectra of CT-DNA with an increasing amount of the *in situ* prepared Cu (II) complexes $\mathbf{2}Cl_2$ and $\mathbf{3}Cl_2$ and their corresponding ligands bimzE and bimzB are shown in Fig. 9 (for complex $\mathbf{1}Cl_2$ and bimzS, see Fig. S11a and b).

In general, a titration of the complexes or the ligands to a DNA solution led to an enhanced alteration of the positive band at 275 nm, whereas the negative band at 245 nm remained unaffected. Thereby, both the complexes $\mathbf{2}Cl_2$ and $\mathbf{3}Cl_2$ caused a more pronounced change in comparison to their corresponding ligands bimzE and bimzB. This suggests intercalation caused by base stacking of the investigated compounds. However, the moderate alteration of the positive band and the fact that intercalation was excluded by UV–VIS and fluorescence spectroscopy, indicate that electrostatic interaction is the dominant DNA binding mode. Groove binding as another possible binding mode derived from DNA melting and EtBr displacement studies, can be excluded based on the CD spectra.

When considering all three DNA binding assays together, we assume a tighter DNA binding for $\mathbf{2}Cl_2$ than for $\mathbf{3}Cl_2$ caused by electrostatic interaction. This is probably due to the more flexible linker moiety in the ligand scaffold bimzE, allowing for easier access to the DNA molecule. Interestingly, $\mathbf{1}Cl_2$ as well as its ligand, showed a pronounced alteration of CD spectra of CT-DNA at even lower concentrations when compared to the other compounds (Fig. S11a and b). This observation might be due to interaction of the disulfide bridge with the biomolecule.

4. Conclusion

In conclusion we synthesized the benzimidazole-based ligands bimzS, bimzE and bimzB and their corresponding Cu(II) complexes $[Cu(bimzE)_2](ClO_4)_2$ ($\mathbf{2}(ClO_4)_2$) and $[Cu(bimzB)_2](NO_3)_2$ ($\mathbf{3}(NO_3)_2$). During synthesis of $[Cu(bimzS)_2](NO_3)_2$ ($\mathbf{1}(NO_3)_2$) a decomposition of the disulfide bridge of the bimzS ligand to benzimidazole was observed, thus all following experiments were carried out with *in situ* prepared metal complex solutions ($\mathbf{1}Cl_2$, $\mathbf{2}Cl_2$, $\mathbf{3}Cl_2$).

Due to the distorted square planar geometry of the Cu(II) complex $\mathbf{2}(ClO_4)_2$ in comparison to the ideal square planar geometry of the Cu (II) complex $\mathbf{3}(NO_3)_2$, a shift of the redox couple Cu(II)/Cu(I) to a higher redox potential was observed. This resulted in a better catalytic generation of ROS and consequently an enhanced nuclease activity. The underlying distortion of the complex geometry, as derived from EPR spectroscopic results, is attributed to the more flexible ligand bimzE in $\mathbf{2}(ClO_4)_2$ with an ethylene bridge in contrast to the rigid ligand bimzB in $\mathbf{3}(NO_3)_2$.

In situ prepared Cu(II) complexes $\mathbf{1}Cl_2$, $\mathbf{2}Cl_2$ and $\mathbf{3}Cl_2$ were tested regarding their nuclease activity towards plasmid DNA pBR322. Under the conditions applied no DNA cleavage activity of complex $\mathbf{1}Cl_2$ was observed. This indicates that the disulfide bridge is involved in redox-based side reactions, which hamper the generation of ROS. Complexes $\mathbf{2}Cl_2$ and $\mathbf{3}Cl_2$ were able to cleave plasmid DNA into its linear form at a complex concentration of 100 µM in the presence of ascorbate. This indicates an oxidative DNA cleavage pathway, which was also proved

in an ROS quenching experiment by the occurrence of hydroxyl radicals and hydrogen peroxide. Overall, complex **2**Cl_2 possesses a better nuclease activity in comparison to **3**Cl_2 due to its flexible linker bridging the two benzimidazole moieties, and thus easy access to the Cu(II)/Cu(I) redox cycle. In accordance with these results, **2**Cl_2 also exhibited the tightest binding to DNA. UV–VIS (DNA melting curves), CD and fluorescence (EtBr displacement assay) spectroscopy indicated electrostatic interaction as a prominent DNA binding mode, which might be favored for the complex with the ligand having the most flexible linker moiety.

Overall, the biological activity towards DNA of the Cu(II) complexes **1–3** with bridged benzimidazole ligands was described for the first time. Redox chemistry and DNA binding, and consequently, oxidative DNA cleavage activity was dependent on the flexibility of the linkage between the benzimidazole moieties.

Acknowledgements

Kathie Coverley Naylor and the Kulak group are acknowledged for proof-reading of this article.

Appendix A. Supplementary data

Supplementary data to this article can be found online at https://doi.org/10.1016/j.jinorgbio.2019.01.016.

References

[1] P.M. van Berkel, D.J. Dijkstra, W.L. Driessen, J. Reedijk, D.C. Sherrington, React. Funct. Polym. 28 (1995) 39–54.
[2] H.J. Hoorn, P. de Joode, W.L. Driessen, J. Reedijk, React. Funct. Polym. 27 (1995) 223–235.
[3] A.O. Patil, S. Zushma, R.T. Stibrany, S.P. Rucker, L.M. Wheeler, J. Polym. Sci. A Polym. Chem. (2003) 2095–2106.
[4] R.T. Stibrany, D.N. Schulz, S. Kacker, A.O. Patil, L.S. Baugh, S.P. Rucker, S. Zushma, E. Berluche, J.A. Sissano, Macromolecules 36 (2003) 8584–8586.
[5] R.T. Stibrany, H.J. Shugar, J.A. Potenza, Acta Crystallogr. E Crystallogr. Commun. 58 (2002) o1142–o1144.
[6] B. Xie, T. Elder, L.J. Wilson, D.M. Stanbury, Inorg. Chem. 38 (1999) 12–19.
[7] M. Gaba, S. Singh, C. Mohan, Eur. J. Med. Chem. 76 (2014) 494–505.
[8] Y. Bansal, O. Silakari, Bioorg. Med. Chem. 20 (2012) 6208–6236.
[9] C.A. Bell, C.C. Dykstra, N.A. Naiman, M. Cory, T.A. Fairly, R.R. Tidwell, Antimicrob. Agents Chemother. 37 (1993) 2668–2673.
[10] R.L. Lombardy, F.A. Tanious, K. Ramachandran, R.R. Tidwell, W.D. Wilson, J. Med. Chem. 39 (1996) 1452–1462.
[11] R.R. Tidwell, S.K. Jones, N.A. Naiman, L.C. Berger, W.B. Brake, C.C. Dykstra, J.E. Hall, Antimicrob. Agents Chemother. 37 (1993) 1713–1716.
[12] N.M. Salunke, V.K. Revankar, V.B. Mahale, Transition Met. Chem. 19 (1994) 53–56.
[13] F. Mancin, P. Scrimin, P. Tecilla, U. Tonellato, Chem. Commun. (2005) 2540–2548.
[14] L. Hocharoen, J.W. Cowan, Chem. Eur. J. 15 (2009) 8670–8676.
[15] Q. Zhou, P. Yang, Inorg. Chim. Acta 359 (2006) 1200–1206.
[16] M. Pitié, G. Pratviel, Chem. Rev. 110 (2010) 1018–1059.
[17] W. Wang, Y.A. Lee, G. Kim, S.K. Kim, G.Y. Lee, J. Kim, Y. Kim, G.J. Park, C. Kim, J. Inorg. Biochem. 153 (2015) 143–149.
[18] K. Suntharalingam, D.J. Hunt, A.A. Duarte, A.J.P. White, D.J. Mann, R. Vilar, Chem. Eur. J. 18 (2012) 15133–15141.
[19] C. Wende, C. Lüdtke, N. Kulak, Eur. J. Inorg. Chem. (2014) 2597–2612.
[20] R. Loganathan, S. Ramakrishnan, E. Suresh, A. Riyasdeen, M.A. Akbarsha, M. Palaniandavar, Inorg. Chem. 51 (2012) 5512–5532.
[21] Q.-M. Jin, Y. Lu, J.-L. Jin, H. Guo, G.-W. Lin, Y. Wang, T. Lu, Inorg. Chim. Acta 421 (2014) 91–99.
[22] Z.A. Al-Mudaris, A.S.A. Majid, D. Ji, A. Al-Mudarris, S.-H. Chen, P.-H. Liang, H. Osman, S.K.K.J. Din, A.M.S.A. Majid, PLoS One 8 (2013) e80983.
[23] Y.-Y. Deng, F.-Q. Liu, Y.-L. Jin, Transition Met. Chem. 37 (2012) 309–314.
[24] G.A. van Albada, W.J.J. Smeets, N. Veldman, A.L. Spek, J. Reedijk, Inorg. Chim. Acta 290 (1999) 105–112.
[25] J.A. VanAllan, B.D. Deacon, Org. Synth. 30 (1950) 56.
[26] K. Ramadas, N. Srinivasan, N. Janarthanan, R. Pritha, Org. Prep. Proced. Int. 28 (1996) 352–355.
[27] G.A. van Albada, M.T. Lakin, N. Veldman, A.L. Spek, J. Reedijk, Inorg. Chem. 34 (1995) 4910–4917.
[28] L. Li, G.J. Clarkson, Org. Lett. 9 (2007) 497–500.
[29] R.P. Hertzberg, P.B. Dervan, Biochemistry 23 (1984) 3934–3945.
[30] C. Fan, C.-B. Ma, M.-Q. Hu, C.-N. Cheng, Q.-T. Liu, Chin. J. Struct. Chem. 25 (2006) 285–289.
[31] Z.L. Cheng, K.W.M. Siu, R. Guevremont, S.S. Berman, Org. Mass Spectrom. 27 (1992) 1370–1376.
[32] C.L. Gatlin, F. Tureček, T. Vaisar, Anal. Chem. 66 (1994) 3950–3958.
[33] B.J. Hathaway, G. Wilkinson, R.D. Gillard, J.A. McCleverty (Eds.), Comprehensive Coordination Chemistry, Vol. 5 Copper, Pergamon Press, Oxford, 1987, pp. 662–673.
[34] G. Tabbì, A. Giuffrida, R.P. Bonomo, J. Inorg. Biochem. 128 (2013) 137–145.
[35] L.K. Mishra, N. Dubey, Acta Cienc. Indica, Chem 21 (1995) 83–85.
[36] F.-f. Jian, H.-x. Wang, H.-l. Xiao, K. Jiao, Chem. Res. Chin. Univ. 21 (2005) 12–16.
[37] L. Guilloreau, S. Combalbert, A. Sournia-Saquet, H. Mazarguil, P. Faller, Chembiochem 8 (2007) 1317–1325.
[38] J. Nagaj, K. Stokowa-Sołtys, E. Kurowska, T. Frączyk, M. Jeżowska-Bojczuk, W. Bal, Inorg. Chem. 52 (2013) 13927–13933.
[39] J. Heinrich, J. Stubbe, N. Kulak, Inorg. Chim. Acta 481 (2018) 79–86.
[40] D. Giustarini, I. Dalle-Donne, R. Colombo, A. Milzani, R. Rossi, Nitric Oxide 19 (2008) 252–258.
[41] C. Rajarajeswari, M. Ganeshpandian, M. Palaniandavar, A. Riyasdeen, M.A. Akbarsha, J. Inorg. Biochem. 140 (2014) 255–268.
[42] M. Sunita, M. Padmaja, B. Anupama, C.G. Kumari, J. Fluoresc. 22 (2012) 1003–1012.
[43] X.-B. Fu, J.-J. Zhang, D.-D. Liu, Q. Gan, H.-W. Gao, Z.-W. Mao, X.-Y. Le, J. Inorg. Biochem. 143 (2015) 77–87.
[44] J.-A. Zhao, H.-B. Yu, S.-C. Zhi, R.-N. Mao, J.-Y. Hu, X.-X. Wang, Chin. Chem. Lett. 28 (2017) 1539–1546.
[45] J. Hu, Y. Guo, J. Zhao, J. Zhang, Bioorg. Med. Chem. 25 (2017) 5733–5742.
[46] F.B. Everling, W. Weis, H. Staudinger, Hoppe Seylers Z. Physiol. Chem. 350 (1969) 886–888.
[47] K.K. Millis, K.H. Weaver, D.L. Rabenstein, J. Org. Chem. 58 (1993) 4144–4146.
[48] M.K. Eberhardt, R. Colina, J. Org. Chem. 53 (1988) 1071–1074.
[49] K. Li, L.-H. Zhou, J. Zhang, S.-Y. Chen, Z.-W. Zhang, J.-J. Zhang, H.-H. Lin, X.-Q. Yu, Eur. J. Med. Chem. 44 (2009) 1768–1772.
[50] E.A. Mazzio, K.F.A. Soliman, Neurochem. Res. 28 (2003) 733–741.
[51] J. Hormann, C. Perera, N. Deibel, D. Lentz, B. Sarkar, N. Kulak, Dalton Trans. 42 (2013) 4357–4360.
[52] Y. Cao, X.-w. He, Spectrochim. Acta A Mol. Biomol. Spectrosc. 54 (1998) 883–892.
[53] S. Roy, A.K. Patra, S. Dhar, A.R. Chakravarty, Inorg. Chem. 47 (2008) 5625–5633.
[54] D.L. Boger, B.E. Fink, S.R. Brunette, W.C. Tse, M.P. Hedrick, J. Am. Chem. Soc. 123 (2001) 5878–5891.
[55] M.R. Eftink, C.A. Ghiron, Anal. Biochem. 114 (1981) 199–227.
[56] A.R. Morgan, J.S. Lee, D.E. Pulleyblank, N.L. Murray, D.H. Evans, Nucleic Acids Res. 7 (1979) 547–565.
[57] W. Yang, X. Chen, H. Su, W. Fang, Y. Zhang, Chem. Commun. 51 (2015) 9616–9619.
[58] X. Sheng, X.-M. Lu, Y.-T. Chen, G.-Y. Lu, J.-J. Zhang, Y. Shao, F. Liu, Q. Xu, Chem. Eur. J. 13 (2007) 9703–9712.
[59] V.I. Ivanov, L.E. Minchenkova, A.K. Schyolkina, A.I. Poletayev, Biopolymers 12 (1973) 89–110.
[60] N. Shahabadi, S. Kashanian, A. Fatahi, Bioinorg. Chem. Appl. 2011 (2011) 687571.
[61] P. Uma Maheswari, M. Palaniandavar, J. Inorg. Biochem. 98 (2004) 219–230.
[62] C. Tong, G. Xiang, Y. Bai, J. Agric. Food Chem. 58 (2010) 5257–5262.